Zero-temperature dynamics of the spherical model with non-reciprocal interactions

Daniel A. Stariolo

Universidade Federal Fluminense, Instituto de Física, Av. Litorânea s/n, Campus da Praia Vermelha, 24210-346 Niterói, RJ, Brazil

Fernando L. Metz

Universidade Federal do Rio Grande do Sul, Instituto de Física, 91501-970 Porto Alegre, RS, Brazil

Abstract. We analytically solve the zero-temperature dynamics of the spherical model with non-reciprocal random interactions drawn from the real elliptic ensemble of random matrices, where a single parameter η continuously interpolates between purely symmetric $(\eta = 1)$ and purely antisymmetric $(\eta = -1)$ couplings. We show that the two-time correlation and response functions depend on both times in the presence of non-reciprocal interactions, reflecting the breakdown of time-translation invariance and the absence of equilibrium at long times. Nevertheless, the long-time relaxation of the two-time observables is governed by exponential decays, in contrast to the slow, power-law relaxation characteristic of the model with purely symmetric interactions. We further show that, when the interactions present antisymmetric correlations of strength $\eta < 0$, there is a time scale $\tau(\eta)$ above which the dynamics undergoes a transition to an oscillatory regime where the two-time observables display periodic oscillations with an exponentially decaying amplitude. Overall, our results give a detailed account of the dynamics of the spherical model with non-reciprocal interactions at zero temperature, providing a benchmark for the study of complex systems with nonlinear and asymmetric interactions.

1. Introduction

In many complex systems, including neural networks [1, 2], ecosystems [3, 4, 5], and epidemic spreading [6], the dynamics of N interacting degrees of freedom $S_1, \ldots S_N$ is described by a set of ordinary differential equations of the form:

$$\frac{dS_i}{dt} = \sum_{j=1}^{N} J_{ij} g(S_i, S_j), \qquad i = 1, \dots N,$$
(1)

where the matrix elements $\{J_{ij}\}_{i,j=1}^N$ define a random network of pairwise coupling strengths, and the model-dependent function $g(S_i, S_j)$ specifies the nature of the interactions between units. In general, $g(S_i, S_j)$ is nonlinear and then solving the

dynamics defined by Eq. (1) for finite N is a formidable task. Significant progress has been achieved in the limit $N \to \infty$ using dynamical mean-field theory [1, 4, 5, 7, 8].

A simplified yet nontrivial model is obtained when $g(S_i, S_j) = S_i$ $(i \neq j)$ and the degrees of freedom satisfy the spherical constraint $\sum_{i=1}^{N} S_i^2 = N$. This spherical model [9] has been extensively studied in the context of spin glasses and, more generally, glassy systems. Beyond its relevance for studying glassy dynamics [10], the spherical model provides a simplified framework to address questions related to the nonequilibrium dynamics of complex systems, including the influence of the interaction matrix on entropy production [11] and the decay of correlations around a trivial fixed-point [2]. Apart from the global spherical constraint, the time evolution of the model is governed by linear differential equations that can be solved exactly using results from random matrix theory [12]. The analytic solution for symmetric Gaussian interactions in the $N \to \infty$ limit was first obtained in the seminal work of [13]. Although the equilibrium properties of the spherical model with symmetric couplings do not display replica symmetry breaking, which underlies the complexity of spin glasses, the dynamical evolution of the two-time correlation and response functions still exhibit the phenomenon of aging [13, 14], a distinctive feature of glassy dynamics. The standard phenomenology of aging includes the breakdown of time-translation invariance and the slow, scaleinvariant relaxation of two-time observables, typically described by a power-law decay. In the aging regime, the relaxation timescale grows with the waiting time elapsed since the preparation of the sample and, in the $N \to \infty$ limit, the system never reaches equilibrium. In models with symmetric couplings, where detailed balance holds, aging effects are attributed to the complex topology of the energy landscape [15], which contains many saddle-points with small curvature that can trap the dynamics for long times.

Recently, there has been renewed interest in the properties of many-body systems with non-reciprocal, asymmetric, or non-Hermitian interactions, both in classical [16, 17, 18, 19, 20, 21, 22, 23, 24, 25, 26, 27, 28, 29, 30 and quantum settings [31, 32, 33, 34, 35, 36. Non-reciprocity is particularly relevant for modeling the interactions in complex systems, leading to dynamical behaviours that have no equilibrium counterpart, including the emergence of oscillations and even chaotic dynamics [37, 17, 20, 8]. The spherical model offers an ideal framework to explore how the relaxation properties of glassy systems are affected by the introduction of non-reciprocal interactions. In a seminal work, Crisanti and Sompolinsky [38] studied the dynamics of the spherical model with a tunable correlation between J_{ij} and J_{ji} , allowing for a systematic analysis of the role of asymmetric coupling strengths. The main result was that any degree of non-reciprocity destroys the spin glass phase at finite temperatures. Moreover, at finite but small temperatures, the dynamics exhibits a characteristic timescale, dependent on the degree of asymmetry in the interactions, below which the system behaves as a frozen spin glass and above which it behaves as a paramagnet [38]. A similar behaviour has been also observed in other spin-glass models, where the crossover from an aging regime to a time-translation invariant dynamics at long timescales has been termed interrupted aging [39, 40, 41, 42].

Although long time aging effects are absent at finite temperatures, it was found in [38] that the model undergoes a transition to a frozen spin-glass state at zero temperature, where the correlation function remains equal to one. However, the results of reference [38] rely on the assumption of time-translation invariance of the two-time correlation and response functions, which by construction excludes any aging behaviour and, more generally, prevents the study of nonequilibrium dynamics. Consequently, the zero-temperature dynamics of the model remains poorly understood, and it is unclear whether the two-time observables exhibit aging.

Building on known results for the eigenvector correlations of non-Hermitian random matrices [43, 44, 2, 45, 46], we analytically solve the zero-temperature dynamics of the spherical model with non-reciprocal interactions. We derive the long-time behaviour of the correlation and response functions and show that time-translation invariance is broken for any nonzero contribution of the symmetric part of the interactions, as the two-time observables depend explicitly on both times. Similarly to the purely symmetric case, the correlation function displays an initial plateau, whose duration increases with both the waiting time and the strength of the symmetric couplings. However, although the model never reaches equilibrium, it does not exhibit slow dynamics: the longtime behaviour of the correlation and response functions is dominated by exponential decays. Furthermore, we show that the asymptotic dynamics undergoes a transition to an oscillatory regime as a function of the parameter controlling the correlation between J_{ij} and J_{ii} . For sufficiently strong antisymmetric interactions, the two-time observables exhibit periodic oscillations with an exponentially decaying amplitude. We compute exactly the period and phase of these oscillations as functions of the waiting time and the correlation parameter. These results close a long-standing gap in our understanding of how non-reciprocal interactions impact the zero-temperature dynamics of the spherical model.

The paper is organized as follows. In section 2 we revisit the definition of the spherical model with non-reciprocal interactions. In section 3, we present the analytic solution of the dynamics for arbitrary system sizes N. In section 4, we discuss our main results for the dynamics of the correlation and response functions in the $N \to \infty$ limit. Section 5 summarizes our main findings and outlines possible directions for future work. In Appendix A we show the derivation of the expressions for the correlation and response for finite-size systems.

2. The spherical model with non-reciprocal interactions

The model is defined in terms of N real-valued spins $S_i(t)$ (i = 1, ..., N) that evolve in time according to the zero-temperature Langevin equations [13]:

$$\frac{\partial S_i(t)}{\partial t} = \sum_{j=1}^N S_j(t)J_{ji} - z(t)S_i(t) + h_i(t), \qquad i = 1, \dots, N,$$
(2)

where $h_i(t)$ are local external fields. The function z(t) ensures that the global spherical constraint:

$$\sum_{i=1}^{N} S_i^2(t) = N \tag{3}$$

is satisfied at any time t. Thus, the global states of the system lie on the surface of an N-1-dimensional hypersphere of radius \sqrt{N} .

The element $J_{ij} \in \mathbb{R}$ of the $N \times N$ interaction matrix J quantifies the strength of the directed coupling $i \to j$, that is, the influence of spin $S_i(t)$ on $S_j(t)$. The diagonal elements of J are set to zero. To study how the introduction of non-reciprocal couplings affects the dynamics, we consider interactions drawn from the real elliptic ensemble of random matrices [47], where the off-diagonal entries of J are identically distributed real Gaussian random variables with mean zero and second moments given by:

$$\langle J_{ij}^2 \rangle = \frac{1}{N}, \qquad \langle J_{ij}J_{ji} \rangle = \frac{\eta}{N}.$$
 (4)

The parameter $\eta \in [-1, 1]$ controls the degree of correlation between J_{ij} and J_{ji} for any distinct pair (i, j) of sites. For $\eta = 0$, J_{ij} and J_{ji} are statistically independent. For $\eta \to 1$, the interactions are symmetric, i.e., $J_{ij} = J_{ji}$. For $\eta \to -1$, $J_{ij} = -J_{ji}$ and we obtain an anti-correlated ensemble of Gaussian random matrices.

In this work, we analytically compute the two-time correlation

$$C_N(t,t') = \frac{1}{N} \sum_{i=1}^{N} S_i(t) S_i(t')$$
(5)

and the response function

$$G_N(t,t') = \frac{1}{N} \sum_{i=1}^{N} \frac{\delta S_i(t)}{\delta h_i(t')} \bigg|_{h=0}$$

$$\tag{6}$$

at time t due to a perturbation at time t' < t. In particular, we aim to understand the fate of the aging behaviour when the interactions become non-reciprocal $(\eta < 1)$, since aging is a distinctive feature of the non-equilibrium dynamics of the model with symmetric couplings [13].

3. Analytical solution of the model dynamics

In the following, we derive extact expressions for the two-time autocorrelations and response functions of the spherical model with asymmetric couplings at zero noise. The results for arbitrary size N hold for arbitrary interaction matrices and initial conditions, setting a starting point for analysing the behaviour of the model dynamics in a wide range of situations. By taking the $N \to \infty$ limit, we derive analytical expressions for the two-time quantities when the interactions are sampled from the real elliptic ensemble. We focus on systems prepared on random initial conditions, with a focus on the fate of the aging behaviour observed in the symmetric case [13, 15].

3.1. Correlation and response for finite-size systems

The linear Eqs. (2) can be solved by decoupling the dynamical variables in terms of the eigenvalues and eigenvectors of the interaction matrix J. Because the interactions can be non-reciprocal, $J \neq J^{\dagger}$, the column (right) eigenvectors of J are not the Hermitian transpose of the row (left) eigenvectors. Thus, J has a set of right eigenvectors, $\{|R_{\alpha}\rangle\}_{\alpha=1,\ldots,N}$, and a set of left eigenvectors, $\{\langle L_{\alpha}|\}_{\alpha=1,\ldots,N}$, which fulfill the equations:

$$J|R_{\alpha}\rangle = \lambda_{\alpha}|R_{\alpha}\rangle, \qquad \langle L_{\alpha}|J = \lambda_{\alpha}\langle L_{\alpha}|,$$
 (7)

where $\lambda_1, \ldots, \lambda_N$ are the complex eigenvalues of J. The left and right eigenvectors form a biorthogonal set

$$\langle L_{\alpha}|R_{\beta}\rangle = \delta_{\alpha\beta},\tag{8}$$

and fulfill the completeness relation

$$\sum_{\alpha=1}^{N} |R_{\alpha}\rangle \langle L_{\alpha}| = \mathbf{I}, \tag{9}$$

where I is the $N \times N$ identity matrix. The eigenvectors within each set are not orthogonal to each other, i.e., $\langle L_{\alpha}|L_{\beta}\rangle \neq 0$ and $\langle R_{\alpha}|R_{\beta}\rangle \neq 0$. Moreover, Eqs. (8) and (9) remain invariant under the rescalings $|R_{\alpha}\rangle \to c_{\alpha} |R_{\alpha}\rangle$ and $\langle L_{\alpha}| \to c_{\alpha}^{-1} \langle L_{\alpha}|$, with $c_{\alpha} \in \mathbb{C}$. This invariance implies that the norm of the left or right eigenvectors can be chosen arbitrarily. Consequently, the dynamical equations for the physical observables must be invariant under such rescaling.

By introducing the global state vector $\langle S(t)| = (S_1(t) \ S_2(t) \dots S_N(t))$, Eq. (2) can be written as:

$$\frac{\partial \langle S(t)|}{\partial t} = \langle S(t)| \mathbf{J} - z(t) \langle S(t)| + \langle h(t)|, \tag{10}$$

with $\langle h(t)| = (h_1(t) \ h_2(t) \dots h_N(t))$. Let us define the projections $r_{\alpha}(t) \in \mathbb{C}$ and $l_{\alpha}(t) \in \mathbb{C}$ of $\langle S(t)|$ onto the eigenvectors:

$$r_{\alpha}(t) = \langle S(t)|R_{\alpha}\rangle$$
 and $l_{\alpha}(t) = \langle S(t)|L_{\alpha}\rangle$. (11)

By multiplying Eq. (10) on the right by $|R_{\alpha}\rangle$ and $|L_{\alpha}\rangle$, it is straightforward to write down dynamical equations for $r_{\alpha}(t)$ and $l_{\alpha}(t)$:

$$\frac{\partial r_{\alpha}(t)}{\partial t} = (\lambda_{\alpha} - z(t)) r_{\alpha}(t) + h_{\alpha}^{(R)}(t), \qquad \alpha = 1, \dots, N,$$
(12)

$$\frac{\partial l_{\alpha}(t)}{\partial t} = \sum_{\beta=1}^{N} \lambda_{\beta} \langle L_{\beta} | L_{\alpha} \rangle r_{\beta}(t) - z(t) l_{\alpha}(t) + h_{\alpha}^{(L)}(t), \qquad \alpha = 1, \dots, N,$$
(13)

where $h_{\alpha}^{(R)}(t)$ and $h_{\alpha}^{(L)}(t)$ are the projections of the external field:

$$h_{\alpha}^{(R)}(t) = \langle h(t)|R_{\alpha}\rangle \quad \text{and} \quad h_{\alpha}^{(L)}(t) = \langle h(t)|L_{\alpha}\rangle.$$
 (14)

Note that, contrary to the symmetric case, the set of dynamical equations depend not only on the eigenvalue spectrum of J but also on the set of right and left eigenvectors. In terms of $r_{\alpha}(t)$ and $l_{\alpha}(t)$, the correlation function reads:

$$C_N(t,t') = \frac{1}{N} \sum_{\alpha=1}^{N} r_{\alpha}(t) l_{\alpha}^*(t'), \tag{15}$$

while the response function is given by

$$G_N(t,t') = \frac{1}{N} \lim_{h \to 0} \sum_{\alpha=1}^{N} \sum_{\beta=1}^{N} \frac{\delta r_{\alpha}(t)}{\delta h_{\beta}(t')} \langle L_{\alpha} | \beta \rangle, \qquad (16)$$

where $\{|\beta\rangle\}_{\beta=1,\dots,N}$ is the standard site basis, with $(|\beta\rangle)_{\gamma} = \delta_{\beta\gamma}$. As expected, Eqs. (15) and (16) are invariant under the rescalings $|R_{\alpha}\rangle \to c_{\alpha} |R_{\alpha}\rangle$ and $\langle L_{\alpha}| \to c_{\alpha}^{-1} \langle L_{\alpha}|$.

By solving Eqs. (12) and (13) and then setting h(t) = 0, one can show that the correlation and response functions are given by:

$$C_N(t,t') = \frac{W_N(t,t')}{\sqrt{W_N(t,t)W_N(t',t')}}$$
(17)

and

$$G_N(t,t') = \sqrt{\frac{W_N(t',t')}{W_N(t,t)}} \frac{1}{N} \text{Tr} \left[e^{J(t-t')} \right] - \frac{1}{N} \frac{\left[W_N(t',t') \right]^{\frac{1}{2}}}{\left[W_N(t,t) \right]^{\frac{3}{2}}} W_N(t,2t-t'), \tag{18}$$

where the two-time function $W_N(t,t')$ reads:

$$W_N(t,t') = \frac{1}{N^2} \sum_{\alpha\beta=1}^N e^{\lambda_\alpha t + \lambda_\beta^* t'} r_\alpha(0) r_\beta^*(0) \langle L_\alpha | L_\beta \rangle.$$
 (19)

The details of the calculations are left to Appendix A. Equations (17), (18) and (19) yield the relaxation properties of the response and correlation functions for finite N, arbitrary interaction matrix J, and arbitrary initial conditions. By numerically diagonalizing J, these equations allow us to study finite size effects on the dynamics of the model. In this work, we will present numerical results for finite N, only to illustrate the approach of the dynamics to its $N \to \infty$ limit, which is the main focus of the present study.

3.2. Correlation and response in the thermodynamic limit

The function $W_N(t,t')$ is the central quantity that governs the dynamics of $C_N(t,t')$ and $G_N(t,t')$. Let us assume that, in the limit $N \to \infty$, $W_N(t,t')$ is self-averaging with respect to the randomness in both the initial condition and the coupling strengths. In mathematical terms, this assumption reads:

$$W(t,t') = \lim_{N \to \infty} NW_N(t,t') = \lim_{N \to \infty} \frac{1}{N} \sum_{\alpha\beta=1}^N e^{\lambda_\alpha t + \lambda_\beta^* t'} \overline{r_\alpha(0) r_\beta^*(0)} \langle L_\alpha | L_\beta \rangle, \qquad (20)$$

where $\overline{(...)}$ represents an average over the initial conditions $\langle S(0)|$. From now on, we consider random initial conditions in which $\langle S(0)|$ is drawn from an uniform probability distribution subject to the constraint $\langle S(0)|S(0)\rangle = N$, with

$$\overline{S_i(0)} = 0$$
 and $\overline{S_i(0)S_j(0)} = \delta_{ij}$. (21)

By explicitly averaging over $\langle S(0)|$, we obtain:

$$W(t,t') = \lim_{N \to \infty} \frac{1}{N} \sum_{\alpha\beta=1}^{N} e^{\lambda_{\alpha}t + \lambda_{\beta}^{*}t'} \langle L_{\alpha} | L_{\beta} \rangle \langle R_{\beta} | R_{\alpha} \rangle.$$
 (22)

If the interaction matrix is symmetric, then $\lambda_{\alpha} = \lambda_{\alpha}^*$ and $\langle L_{\alpha}|L_{\beta}\rangle = \langle R_{\beta}|R_{\alpha}\rangle = \delta_{\alpha\beta}$. Thus, as previously observed, the main difference between symmetric and asymmetric interactions is that in the former case the behavior of W(t,t') is independent of the eigenvectors, whereas for asymmetric couplings it depends on both the left and right eigenvectors. This difference arises from the non-orthogonality of the left and right eigenvectors within their respective spaces.

Equation (22) depends on the $N \times N$ matrix of eigenvector overlaps,

$$O_{\alpha\beta} = \langle L_{\alpha} | L_{\beta} \rangle \langle R_{\beta} | R_{\alpha} \rangle, \qquad \alpha, \beta = 1, \dots, N,$$
 (23)

which was originally introduced in [43]. By using the Dirac- δ distribution $\delta^2(z) = \frac{1}{2}\delta(\text{Re}z)\delta(\text{Im}z)$ in the complex plane, we can rewrite Eq. (22) as:

$$W(t,t') = \frac{1}{4} \int d^2 z_1 \int d^2 z_2 \ D(z_1, z_2) \ e^{z_1 t + z_2^* t'}, \tag{24}$$

where $d^2z = dzdz^* = 2 d\text{Re}z d\text{Im}z$. The two-point function $D(z_1, z_2)$ is defined as:

$$D(z_1, z_2) = \lim_{N \to \infty} \frac{4}{N} \sum_{\alpha, \beta = 1}^{N} O_{\alpha\beta} \, \delta^2(z_1 - \lambda_\alpha) \delta^2(z_2 - \lambda_\beta). \tag{25}$$

It quantifies the correlations between eigenvectors at two distinct points, z_1 and z_2 , in the complex plane. In the limit $N \to \infty$, Eqs. (17) and (18) converge to:

$$C(t,t') = \frac{W(t,t')}{\sqrt{W(t,t)W(t',t')}}$$
(26)

and

$$G(t,t') = \sqrt{\frac{W(t',t')}{W(t,t)}} \int_{-\infty}^{\infty} dx \, dy \, \rho(x,y) \, e^{(x+iy)(t-t')}, \tag{27}$$

where $\rho(x,y)$ is the spectral density of \boldsymbol{J} at z=x+iy. Equations (26) and (27) govern the zero-temperature dynamics of the correlation and response functions in the thermodynamic limit for arbitrary interaction matrices \boldsymbol{J} and random initial conditions. The functions C(t,t') and G(t,t') are entirely determined by the spectral properties of \boldsymbol{J} through $D(z_1,z_2)$ and $\rho(x,y)$.

Let us now present the equations for C(t,t') and G(t,t') corresponding to the elliptic random-matrix model for the non-reciprocal interactions. For random interaction matrices J sampled from the real Gaussian elliptic ensemble, defined through Eq. (4),

the eigenvalues are uniformly distributed inside an ellipse in the complex plane, and the spectral density reads [48, 47]

$$\rho(x,y) = \frac{1}{\pi(1-\eta^2)} \Theta \left[1 - \left(\frac{x^2}{(1+\eta)^2} + \frac{y^2}{(1-\eta)^2} \right) \right], \tag{28}$$

with $\Theta(...)$ denoting the Heaviside step function. Moreover, the analytic expression for the two-point eigenvector correlator $D(z_1, z_2)$ has been determined in previous works [43, 44, 49]. Without loss of generality, from now on we set $t' = t_w$ and $t = t_w + \tau$, where t_w is the waiting time and τ the elapsed time. Building on the random-matrix analytic results of [47, 43, 2], we obtain

$$C(t_w + \tau, t_w) = \frac{W(t_w + \tau, t_w)}{\sqrt{W(t_w + \tau)W(t_w)}}$$
(29)

and

$$G(t_w + \tau, t_w) = \sqrt{\frac{W(t_w)}{W(t_w + \tau)}} \frac{I_1(2\sqrt{\eta}\tau)}{\sqrt{\eta}\tau},$$
(30)

where $I_n(x)$ is the modified Bessel function of the first kind. The two-time function $W(t_w + \tau, t_w)$ is given by

$$W(t_{w} + \tau, t_{w}) = (1 + \eta^{2}) I_{0} \left[\psi(t_{w}, \tau) \right] - 2\eta \left[1 + \frac{2(1 - \eta)^{2} \tau^{2}}{\left(\psi(t_{w}, \tau) \right)^{2}} \right] I_{2} \left[\psi(t_{w}, \tau) \right]$$
$$- \frac{1}{t_{w}(t_{w} + \tau)} \sum_{k=1}^{\infty} \eta^{k} k^{2} I_{k} \left(2t_{w} \sqrt{\eta} \right) I_{k} \left(2(t_{w} + \tau) \sqrt{\eta} \right), \tag{31}$$

with

$$\psi(t_w, \tau) = 2\sqrt{\eta \tau^2 + (1+\eta)^2 t_w(t_w + \tau)}.$$
(32)

The one-time function W(t) = W(t,t) follows by setting $\tau = 0$ in Eq. (31):

$$W(t) = (1 + \eta^2)I_0(2(1+\eta)t) - 2\eta I_2(2(1+\eta)t) - \frac{1}{t^2} \sum_{k=1}^{\infty} \eta^k k^2 I_k^2(2t\sqrt{\eta}).$$
 (33)

Equations (29) and (30) enable to perform a detailed analysis of how the symmetry parameter η influences the dynamics of the spherical model defined in Eq. (2).

Setting $\eta = 1$ in Eq. (31) and using properties of the Bessel functions, we obtain

$$W(t_w + \tau, t_w) = \frac{I_1 \left[2 \left(2t_w + \tau \right) \right]}{2t_w + \tau} \quad \text{and} \quad W(t) = \frac{I_1 \left(4t \right)}{2t}, \tag{34}$$

recovering well-known analytic results for symmetric interactions [13], namely

$$C(t_w + \tau, t_w) = \frac{I_1 \left[2 \left(2t_w + \tau \right) \right]}{\sqrt{I_1 \left(4t_w \right) I_1 \left[4(t_w + \tau) \right]}} \frac{\sqrt{4t_w \left(t_w + \tau \right)}}{\left(2t_w + \tau \right)}$$
(35)

and

$$G(t_w + \tau, t_w) = \sqrt{\frac{(t_w + \tau) I_1(4t_w)}{t_w I_1 [4(t_w + \tau)]}} \frac{I_1(2\tau)}{\tau}.$$
(36)

These expressions exhibit aging behaviour in the regime $t, t_w \to \infty$, with $0 < t_w/t < 1$. For arbitrary $\eta < 1$, the behaviour of the correlation and response is qualitatively different from the symmetric case, as we will show in the next section.

4. Results

In this section, we analyze the effect of the symmetry parameter η on the dynamics of $C(t_w + \tau, t_w)$ and $G(t_w + \tau, t_w)$, in the limit $N \to \infty$. Since the long-time dynamics is qualitatively different depending on whether $\eta > 0$ or $\eta < 0$, we analyze the two regimes separately.

4.1. Regime $0 \le \eta \le 1$

Figure 1 shows $C(t_w + \tau, t_w)$ as a function of τ obtained by numerically computing the autocorrelation from Eqs. (29) and (31)-(33). Similarly to the behaviour of the model with symmetric couplings, $\eta = 1$, the behaviour of $C(t_w + \tau, t_w)$ for $0 \le \eta < 1$ depends on both times, t_w and τ . For fixed η (Figure 1(a)), the system remains frozen in the initial state and the correlation exhibits a plateau at $C(t_w + \tau, t_w) = 1$ whose duration increases with t_w , until the system finally relaxes for large enough τ . Fig. 1(b) illustrates how η affects the relaxation of $C(t_w + \tau, t_w)$ at fixed t_w . As η decreases, the length of the plateau also decreases. However, the most pronounced effect of asymmetry in the coupling strengths appears in the decay of $C(t_w + \tau, t_w)$ for large τ . While for $\eta = 1$ the correlation decays as a power-law, for $\eta < 1$ this decay is much faster, exponential in τ . In summary, the phenomenology remains qualitatively similar to the symmetric case: the correlation exhibits a plateau for $\tau \ll t_w$, whose duration is controlled by t_w and η ; the system then leaves the plateau and attains an asymptotic regime for $\tau \gg t_w$, strongly influenced by η . However, unlike the symmetric case, for $\eta < 1$ the long-time dynamics is exponential in τ , as will be shown in the following.

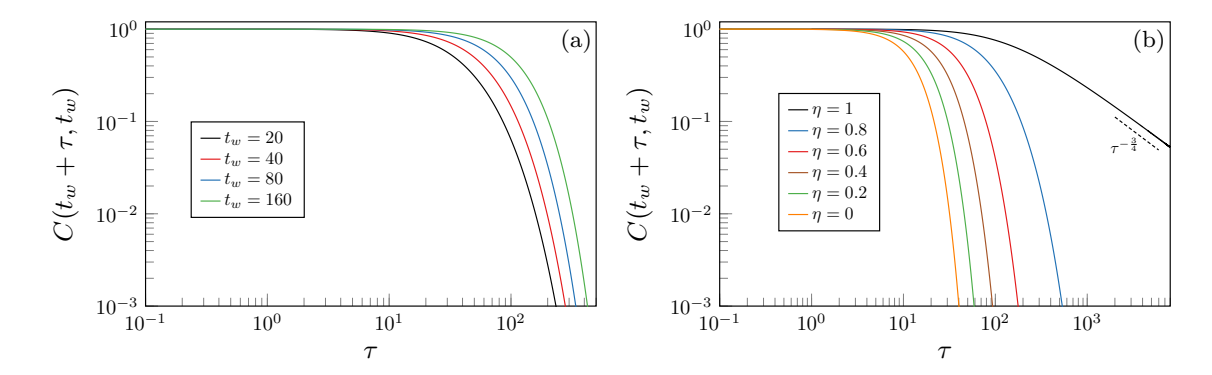


Figure 1. Autocorrelation function $C(t_w + \tau, t_w)$ of the spherical model with non-reciprocal interactions drawn from the elliptic ensemble of random matrices with symmetry parameter η (see Eq. (4)). These results are obtained by numerically computing $C(t_w + \tau, t_w)$ from Eqs. (29) and (31)-(33), which are valid in the $N \to \infty$ limit. (a) $\eta = 0.7$ and different values of the waiting time t_w . (b) $t_w = 40$ and different η .

Let us now characterize the asymptotic behaviour of $C(t_w + \tau, t_w)$ for large t_w and different regimes of τ .

- For $\tau/t_w \to 0$, it is straightforward to show from Eqs. (29) and (31)-(33) that $C(t_w + \tau, t_w) \to 1$. This corresponds to the plateau regime shown in Fig. 1.
- Consider now the time scales where $t_w \gg 1$ and $\tau \gg 1$, with $0 < t_w/\tau \ll 1$. This corresponds to the long-time asymptotic regime in Fig. 1(b), where the decay of the correlation function strongly depends on the symmetry parameter η . For $\eta = 1$, one can show from Eq. (35) that $C(t_w + \tau, t_w)$ exhibits aging behaviour, with the power-law decay [13]:

$$C(t_w + \tau, t_w) \simeq 2\sqrt{2} \left(\frac{t_w}{\tau}\right)^{\frac{3}{4}}, \qquad 0 < t_w/\tau \ll 1.$$
 (37)

For $0 < \eta < 1$, however, the correlation decays in the form:

$$C(t_w + \tau, t_w) \simeq \left[\frac{(1+\eta)^2}{\eta} \frac{t_w}{\tau} \right]^{\frac{5}{4}} \exp\left[-r(\eta)\tau\right], \quad 0 < t_w/\tau \ll 1, \quad (38)$$

with the symmetry-dependent rate

$$r(\eta) = \left(1 - \frac{(1+\eta)}{\sqrt{\eta}} \frac{t_w}{\tau}\right) (1 - \sqrt{\eta})^2. \tag{39}$$

Equation (38) is derived by expanding Eq. (32) for

$$\tau \gg \frac{(1+\eta)}{\sqrt{\eta}} t_w,\tag{40}$$

which defines the time scale for the onset of the exponential decay. Since the limit $\eta \to 0$ of Eq. (38) is singular, the case of $\eta = 0$ must be analyzed separately, as will be discussed below. As $\eta \to 1$, the characteristic time for the decay of correlations, $1/r(\eta)$, diverges, indicating the breakdown of the exponential regime.

Next, we study the dynamics of the response function $G(t_w + \tau, t_w)$. Figure 2 shows $G(t_w + \tau, t_w)$ as a function of τ obtained by numerically evaluating $G(t_w + \tau, t_w)$ from Eqs. (30) and (33). For small τ the curves for different t_w collapse, and $G(t_w + \tau, t_w)$ depends only on τ . For large τ , the curves for different t_w split, showing that $G(t_w + \tau, t_w)$ exhibits a weak dependence on the waiting time. Fig. 2(b) illustrates the strong effect of η on the long-time behaviour of $G(t_w + \tau, t_w)$. For symmetric interactions ($\eta = 1$) and sufficiently large τ , $G(t_w + \tau, t_w)$ decays as a power-law, whereas for $0 < \eta < 1$, the response shows an exponential decay for large τ .

• For $\tau/t_w \to 0$, $G(t_w + \tau, t_w)$ presents a time-translation invariant regime,

$$G(t_w + \tau, t_w) = e^{-(1+\eta)\tau} \frac{I_1(2\sqrt{\eta}\tau)}{\sqrt{\eta}\tau},$$
(41)

as illustrated in Fig. 2(a). Setting $\eta = 1$ in Eq. (41), we recover the expression in [13].

• Consider now the time scales in which $t_w \gg 1$ and $\tau \gg 1$, with $t_w/\tau \ll 1$. For $\eta = 1$, $G(t_w + \tau, t_w)$ displays the power-law decay [13]

$$G(t_w + \tau, t_w) \simeq \frac{1}{\sqrt{4\pi}} (t_w \tau)^{-3/4}, \quad 0 < t_w / \tau \ll 1,$$
 (42)

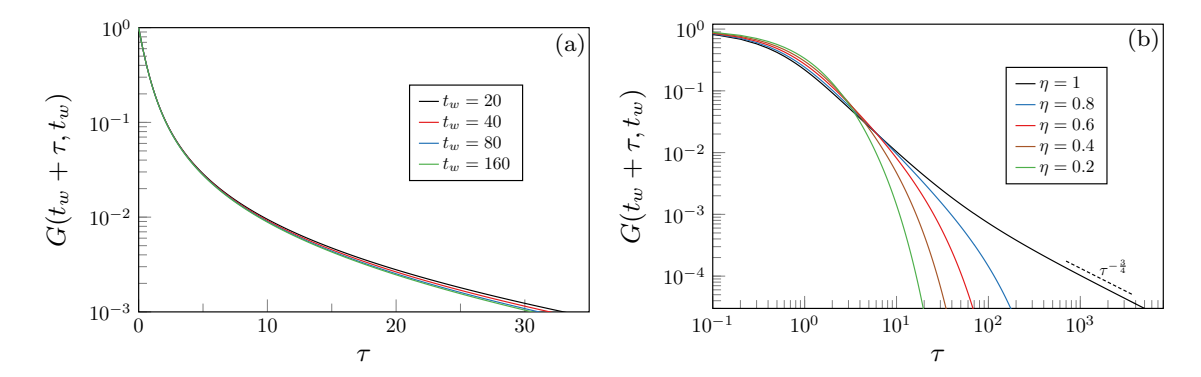


Figure 2. Response function $G(t_w + \tau, t_w)$ of the spherical model with non-reciprocal interactions drawn from the elliptic ensemble of random matrices with symmetry parameter η (see Eq. (4)). These results are obtained by numerically computing $G(t_w + \tau, t_w)$ from Eqs. (30) and (33), which are valid in the thermodynamic limit. (a) $\eta = 0.7$ and different values of t_w . (b) $t_w = 40$ and different η .

whereas for $0 < \eta < 1$ we find

$$G(t_w + \tau, t_w) \simeq \frac{1}{\sqrt{4\pi}} (\eta t_w \tau)^{-1/4} \frac{e^{-(1-\sqrt{\eta})^2 \tau}}{\tau}, \quad 0 < t_w/\tau \ll 1.$$
 (43)

This behaviour is illustrated in Fig. 2. The absence of an exponential prefactor in t_w (present in the corresponding result for the autocorrelation, see. Eqs. (38) and (39)) reflects the weak dependence of $G(t_w + \tau, t_w)$ on the waiting time. For $\eta = 1$, Eq. (43) reduces to a power law decay with an exponent different from that in Eq. (42).

Now we discuss the behaviour of the correlation and response functions for $\eta = 0$. In this case, from Eqs. (31) and (33), the correlation and response are given by:

$$C(t_w + \tau, t_w) = \frac{I_0 \left(2\sqrt{t_w(t_w + \tau)}\right)}{\sqrt{I_0 (2t_w) I_0 (2(t_w + \tau))}}$$
(44)

and

$$G(t_w + \tau, t_w) = \sqrt{\frac{I_0(2t_w)}{I_0(2(t_w + \tau))}}.$$
(45)

Let us analyze the asymptotic regimes of $C(t_w + \tau, t_w)$ and $G(t_w + \tau, t_w)$ for large t_w .

- For $\tau/t_w \to 0$, the dynamics is time-translation invariant, with $C(t_w + \tau, t_w) = 1$ and $G(t_w + \tau, t_w) = e^{-\tau}$.
- On the other hand, when t_w and τ are both large, such that $0 < t_w/\tau \ll 1$, the correlation and response exhibit the leading behaviours:

$$C(t_w + \tau, t_w) \simeq e^{-\left(1 + \frac{2t_w}{\tau} - 2\sqrt{\frac{t_w}{\tau}}\right)\tau},\tag{46}$$

$$G(t_w + \tau, t_w) \simeq \left(\frac{\tau}{t_w}\right)^{\frac{1}{4}} e^{-\tau}, \qquad 0 < t_w/\tau \ll 1.$$
 (47)

We conclude this subsection by comparing our analytic results for $N \to \infty$, Eqs. (29) and (30), with finite-size results derived from Eqs. (17) and (18), obtained through the numerical computation of the eigenvalues and eigenvectors of the interaction matrix for fixed N. Although finite size effects are significant for large τ , Fig. 3 shows that the numerical data systematically approach the theoretical predictions as N increases, thereby confirming our analytic findings for $C(t_w + \tau, t_w)$ and $G(t_w + \tau, t_w)$ in the $N \to \infty$ limit.

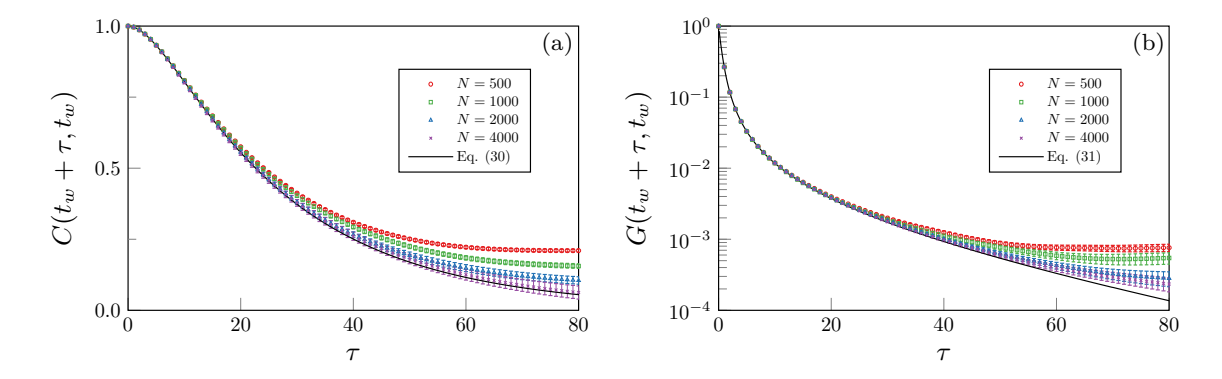


Figure 3. Comparison between numerical results, obtained from Eqs. (17) and (18) for different system sizes N, and the analytical expressions for the correlation and response functions in the limit $N \to \infty$ for $\eta = 0.7$ and $t_w = 10$. The error bars in the numerical data represent the standard deviation of the empirical average computed over a large number of independent realizations.

4.2. Regime $-1 < \eta < 0$

In this regime the antisymmetric part of the interactions is dominant. We first consider the limiting case $\eta = -1$ of purely antisymmetric couplings, where Eq. (32) reduces to $\psi = 2i\tau$. Using the property $I_n(ix) = i^k J_n(x)$, with $J_n(x)$ denoting the Bessel function of order n, one can show that Eqs. (29)-(31) reduce to:

$$C(t_w + \tau, t_w) = G(t_w + \tau, t_w) = \frac{J_1(2\tau)}{\tau}.$$
 (48)

For large τ , the leading term of Eq. (48) reads:

$$C(t_w + \tau, t_w) = G(t_w + \tau, t_w) \simeq \frac{1}{\sqrt{\pi}\tau^{3/2}} \cos\left(2\tau - \frac{3\pi}{4}\right).$$
 (49)

Thus, for $\eta = -1$, the model exhibits a time translation invariant dynamics with periodic oscillations, whose amplitude decays as a power-law.

We now focus on the regime $-1 < \eta < 0$. First, we examine the form of the functions W(t) and $W(t_w + \tau, t_w)$ for negative η . From Eq. (33), we obtain:

$$W(t) = (1 + \eta^2)I_0\left[2(1 - |\eta|)t\right] + 2|\eta|I_2\left[2(1 - |\eta|)t\right] - \frac{1}{t^2} \sum_{k=1}^{\infty} |\eta|^k k^2 J_k^2 \left(2t\sqrt{|\eta|}\right).$$
 (50)

The two-time function $W(t_w + \tau, t_w)$ depends on $\psi(t_w, \tau)$, Eq. (32), which can be real or purely imaginary depending on the relation between τ and t_w . There is a characteristic time:

$$\tau_* = \frac{(1 - |\eta|)}{|\eta|} t_w,\tag{51}$$

obtained from the condition $\psi(t_w, \tau) = 0$, which marks the onset of oscillatory dynamics in the correlation function. For $\tau < \tau_*$, the argument of the square root in Eq. (32) is positive, and the behaviour of Eq. (31) is mainly governed by the modified Bessel functions $I_n(x)$, particularly for large t_w . Consequently, $C(t_w + \tau, t_w)$ exhibits a transient, non-oscillatory dynamics for $\tau < \tau_*$. In contrast, for $\tau > \tau_*$, the argument in Eq. (32) becomes negative, $\psi(t_w, \tau)$ is purely imaginary, and Eq. (31) takes the form:

$$W(t_w + \tau, t_w) = (1 + \eta^2) J_0 \left(2\sqrt{\phi} \right) - 2|\eta| \left[1 - \frac{(1 + |\eta|)^2 \tau^2}{2\phi} \right] J_2 \left(2\sqrt{\phi} \right)$$

$$- \frac{1}{t_w(t_w + \tau)} \sum_{k=1}^{\infty} |\eta|^k k^2 J_k \left(2t_w \sqrt{|\eta|} \right) J_k \left(2(t_w + \tau) \sqrt{|\eta|} \right),$$
(52)

with

$$\phi = |(1 - |\eta|)^2 t_w(t_w + \tau) - |\eta|\tau^2|. \tag{53}$$

Equation (52), given only in terms of Bessel functions $J_n(x)$, leads to an oscillatory dynamics of $C(t_w + \tau, t_w)$ for $\tau > \tau_*$. Note that the characteristic time τ_* shows the limiting behaviours $\tau_* \to 0$ and $\tau_* \to \infty$ for $|\eta| \to 1$ and $|\eta| \to 0$, respectively.

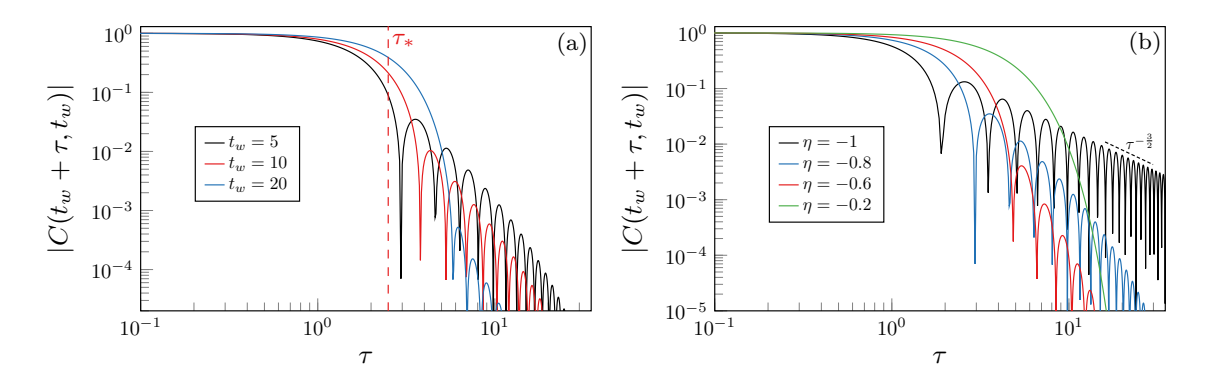


Figure 4. Absolute value of the autocorrelation function of the spherical model with non-reciprocal interactions drawn from the real elliptic ensemble of random matrices with symmetry parameter $\eta < 0$. These results are obtained by numerically computing $|C(t_w + \tau, t_w)|$ from Eqs. (29), (50) and (52), which are valid in the $N \to \infty$ limit. (a) $\eta = -0.8$ and different values of t_w . The vertical dashed line indicates the characteristic time τ_* , Eq. (51), which marks the onset of oscillations for $t_w = 10$. (b) $t_w = 5$ and different values of $\eta < 0$.

Figure 4 shows the relaxation of the absolute value of the autocorrelation as a function of τ , obtained from Eq. (29) for negative η . We note that, for $-1 < \eta < 0$, the dynamics of $C(t_w + \tau, t_w)$ is not time-translation invariant, as was the case for positive η values. The duration of the short initial plateau, $C(t_w + \tau, t_w) \simeq 1$, slightly increases with

 t_w , while the functional form of $|C(t_w + \tau, t_w)|$ describing the non-oscillatory decay up to $\tau = \tau_*$ seems qualitatively similar to the results for $0 < \eta < 1$ (see Fig. 1). For $\tau > \tau_*$, the system enters the oscillatory regime, with an amplitude that decays faster than a power-law. Fig. 4(b) illustrates how $\eta < 0$ influences the relaxation of $|C(t_w + \tau, t_w)|$. As $|\eta|$ increases, the duration of the plateau decreases until it disappears at $\eta = -1$, where the characteristic time τ_* vanishes and the oscillatory dynamics becomes time-translation invariant. For $\eta = -1$, the amplitude decays as a power-law, analogous to the slow dynamics observed at the opposite limit $\eta = 1$.

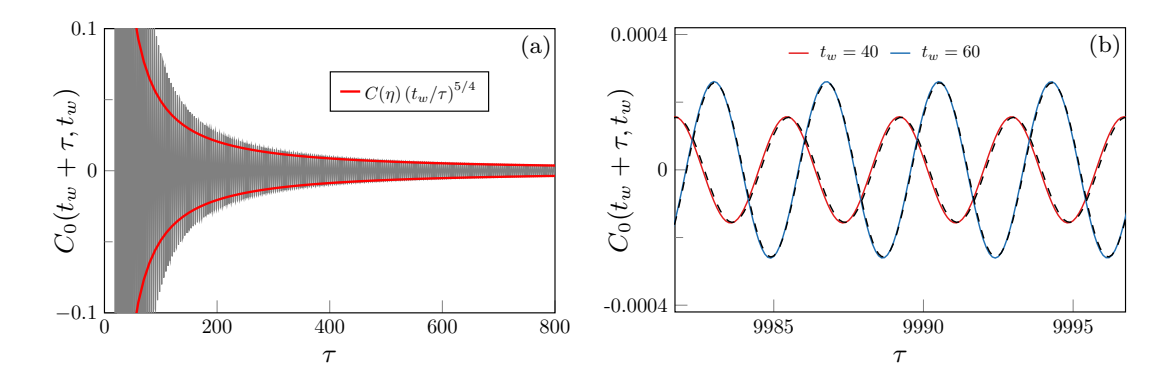


Figure 5. Rescaled correlation function $C_0(t_w + \tau, t_w)$ for negative η . These results are obtained by numerically computing $C_0(t_w + \tau, t_w)$ from Eqs. (29) and (57). (a) $C_0(t_w + \tau, t_w)$ for $\eta = -0.7$ and $t_w = 40$. The solid red lines show the analytic result for the amplitude extracted from Eqs. (54) and (57). (b) Long-time periodic oscillations of $C_0(t_w + \tau, t_w)$ for $\eta = -0.7$ and two values of t_w . The dashed lines are the analytic prediction of Eq. (54).

It is clear from Fig. 4 that the correlation function exhibits a plateau $C(t_w + \tau, t_w) = 1$ for $\tau/t_w \to 0$. However, the distinctive feature of the dynamics for negative η is the long-time oscillatory behaviour, which we now characterize analytically. For large t_w and $\tau \gg \tau_*$, the correlation decays as:

$$C(t_w + \tau, t_w) \simeq C(\eta) \left(\frac{t_w}{\tau}\right)^{\frac{5}{4}} e^{-2(1-|\eta|)t_w - (1-|\eta|)\tau} \cos\left[2\sqrt{|\eta|}\tau - \xi(t_w, \eta)\right],\tag{54}$$

with the phase:

$$\xi(t_w, \eta) = \frac{(1+\eta)^2}{\sqrt{|\eta|}} t_w + \frac{5\pi}{4}$$
 (55)

and the prefactor:

$$C(\eta) = 2\sqrt{\frac{1+\eta}{\sqrt{|\eta|}}} \frac{(1+\eta)^2}{|\eta|}.$$
 (56)

Therefore, for fixed $t_w \gg 1$, the correlation oscillates with period $T = \pi/\sqrt{|\eta|}$, phase $\xi(t_w, \eta)$, and an amplitude that decreases as $\tau^{-5/4}e^{-(1-|\eta|)\tau}$. To numerically verify the analytical prediction of Eq. (54), it is convenient to introduce the rescaled function:

$$C_0(t_w + \tau, t_w) = e^{2(1-|\eta|)t_w + (1-|\eta|)\tau} C(t_w + \tau, t_w), \tag{57}$$

where $C(t_w + \tau, t_w)$ is computed from Eq. (29). Figure 5 illustrates the oscillatory behaviour of $C_0(t_w + \tau, t_w)$, showing that the amplitude follows the power-law $C(\eta) \left(\frac{t_w}{\tau}\right)^{\frac{5}{4}}$ for sufficiently large τ . Fig. 5(b) displays in more detail the long-time periodic dynamics of $C_0(t_w + \tau, t_w)$, fully confirming Eq. (54) and the analytic expressions for both the period and the phase of oscillations. We note that, as the degree of antisymmetry in the couplings decreases ($|\eta| \to 0$), the oscillations become slower. The phase $\xi(t_w, \eta)$ is also determined by the waiting time t_w , which sets the initial time from which the correlation is computed.

Let us now examine the response function $G(t_w + \tau, t_w)$ for negative η . Its behaviour is illustrated in figure 6. For $\eta = -1$, the dynamics is time-translation invariant and the amplitude of oscillations decays as a power-law (see Eq. (49)). Figure 6(a) shows that, for $-1 < \eta < 0$, $G(t_w + \tau, t_w)$ displays a very weak dependence on t_w , analogous to its behaviour for $0 < \eta < 1$. For $\tau/t_w \to 0$, the response decays as

$$G(t_w + \tau, t_w) = e^{-(1-|\eta|)\tau} \frac{J_1\left(2\sqrt{|\eta|}\tau\right)}{\sqrt{|\eta|}\tau},\tag{58}$$

which corresponds to a time-translation invariant regime. In contrast, for $t_w \gg 1$ and $t_w/\tau \ll 1$, the asymptotic behaviour of $G(t_w + \tau, t_w)$ depends explicitly on t_w ,

$$G(t_w + \tau, t_w) \simeq A(\eta) t_w^{-\frac{1}{4}} \tau^{-\frac{5}{4}} e^{-(1-|\eta|)\tau} \cos\left(2\sqrt{|\eta|}\tau - \frac{3\pi}{4}\right),$$
 (59)

with

$$A(\eta) = \frac{1}{\sqrt{\pi |\eta| \sqrt{|\eta|}}}.$$
(60)

Hence, the response exhibits periodic oscillations with a constant phase, independent of t_w , at variance with Eq. (55). The function $G(t_w + \tau, t_w)$ oscillates with the same period $T = \pi/\sqrt{|\eta|}$ as $C(t_w + \tau, t_w)$, and its amplitude decays as $\tau^{-\frac{5}{4}}e^{-(1-|\eta|)\tau}$ for fixed $t_w \gg 1$. Equation (59) contains no exponential prefactor in t_w , which explains the weak dependence on t_w observed in Fig. 6(a).

We end this subsection by comparing our analytical expressions for $C(t_w + \tau, t_w)$ and $G(t_w + \tau, t_w)$ with finite-size numerical results in the case of negative η . Figure 7 shows the dynamics of the correlation and response for $N \to \infty$, together with numerical results obtained from Eqs. (17) and (18). For $\eta < 0$, finite-size effects are very weak, and the numerical data exhibit an excellent agreement with the analytical predictions of Eqs. (29) and (30) for sufficiently large N.

5. Summary and discussion

The spherical model with non-reciprocal interactions characterized by a symmetry parameter $-1 \le \eta \le 1$ was first studied long ago by Crisanti and Sompolinsky [38]. Their results showed that introducing asymmetric couplings ($|\eta| < 1$) suppresses aging at finite temperatures, leading to a time-translation invariant dynamics. However,

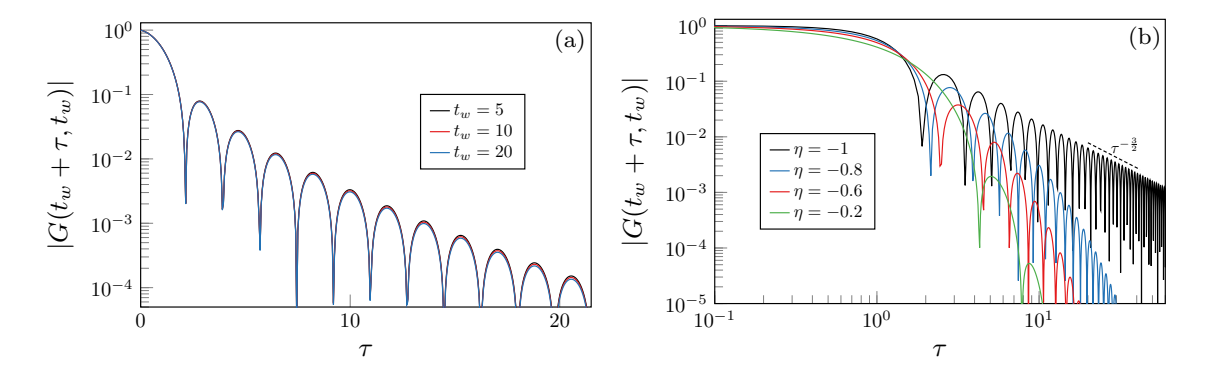


Figure 6. Absolute value of the response function of the spherical model with non-reciprocal interactions drawn from the real elliptic ensemble with symmetry parameter $\eta < 0$. These results are obtained by numerically computing $|G(t_w + \tau, t_w)|$ from Eqs. (30), (50) and (52), which are valid in the $N \to \infty$ limit. (a) $\eta = -0.8$ and different t_w . (b) $t_w = 20$ and different values of $\eta < 0$.

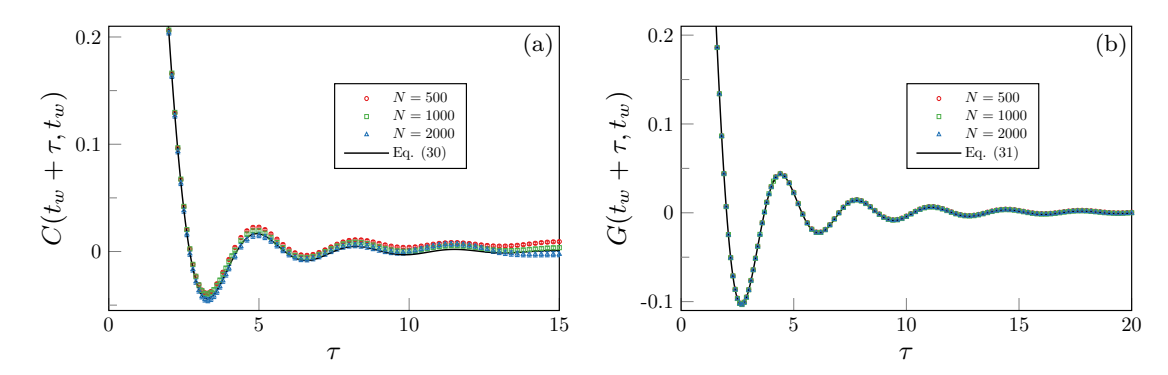


Figure 7. Comparison between numerical results, obtained from Eqs. (17) and (18) for different system sizes N, and the analytical expressions for the correlation and response functions in the limit $N \to \infty$, for $\eta = -0.9$ and $t_w = 10$. The error bars represent the standard deviation of the empirical average computed over a large number of independent realizations.

the possibility that nontrivial dynamical effects could persist at zero temperature has remained open since then. In this work, we have addressed this issue and solved the nonequilibrium dynamics of the spherical model with non-reciprocal interactions at zero temperature, showing that for random initial conditions the long-time behaviour never settles into a time translation-invariant regime for any $|\eta| < 1$.

By analytically computing the two-time autocorrelation and response functions in the thermodynamic limit, we have found that the two-time observables depend explicitly on both times. The relaxation of the correlation function is qualitatively similar to the standard picture observed for purely symmetric interactions [13]: for large waiting times t_w , defining the elapsed time since the preparation of the sample, the correlation exhibits an initial plateau whose duration increases with both t_w and η . However, unlike the power-law relaxation of the two-time observables at $\eta = 1$, the long-time behaviour of the correlation and response functions of the spherical model is governed, for any $|\eta| < 1$,

by an exponential decay with an algebraic prefactor. This is an important difference of the spherical model with non-reciprocal interactions with respect to the slow dynamics characteristic of the symmetric case.

We have also shown that the long-time behaviour of both the correlation and response functions undergoes a transition to an oscillatory regime at $\eta=0$. For $0 \le \eta < 1$, the dynamics of the two-time observables does not exhibit any oscillatory behaviour. For $-1 < \eta < 0$, that is, when the antisymmetric part of the interactions becomes sufficiently strong, the two-time observables display periodic oscillations beyond a characteristic elapsed time $\tau^*(\eta, t_w)$, with a period and phase determined by t_w and η . Recent works by Garcia Lorenzana and co-workers [25, 26, 30] have shown that a spherical model composed of two groups of spins globally coupled to each other through antisymmetric interactions also undergoes a transition to an oscillatory regime. The main difference between our results and theirs lies essentially in the amplitude of oscillations. While in the spherical model the amplitude is governed by an exponential decay, in the Lorenzana model it follows a power-law decay, characteristic of aging.

The slow dynamics of the spherical model with symmetric interactions is commonly attributed to a complex energy landscape [15], in which the number of saddle-points scales with the system size N. It is then natural to expect that the number of stationary states of the model with non-reciprocal interactions play an important role in its dynamical behaviour. From Eq. (1), the stationary states, $\langle S(t)| = \langle S_{\rm st}|$, satisfy:

$$\langle S_{\rm st} | \mathbf{J} = z_{\rm st} \langle S_{\rm st} |,$$
 (61)

where the Lagrange multiplier at the stationary states reads:

$$z_{\rm st} = \frac{1}{N} \left\langle S_{\rm st} | \boldsymbol{J} | S_{\rm st} \right\rangle. \tag{62}$$

By normalizing the left eigenvectors of the interaction matrix J as $\langle L_{\alpha}|L_{\alpha}\rangle = N$, one finds that Eqs. (61) and (62) admit the solutions:

$$\langle S_{\text{st},\alpha} | = \langle L_{\alpha} |, \qquad \alpha = 1, \dots, N,$$
 (63)

with $z_{\text{st},\alpha} = \lambda_{\alpha}$. Thus, there are in total N solutions of Eqs. (61) and (62), although not all of them correspond to physical states. Indeed, since the components of $\langle S_{\text{st}}|$ must be real, only those solutions associated with real eigenvalues $\lambda_{\alpha} \in \mathbb{R}$ represent physical states. It is known that the average number of real eigenvalues of matrices J drawn from the elliptic ensemble scales as \sqrt{N} for large N [50, 51]. Thus, as soon as the antisymmetric part of the interactions is introduced, there is a drastic reduction in the number of stationary states of the model (see also [52]). These stationary points are expected to be sparsely distributed over the surface of the hypersphere, which may lead to a faster relaxation compared with the symmetric case. Studying the stability of these fixed points and their relation to the dynamics of the spherical model is an interesting direction of future work.

Finally, we point out that, in the crossover regime of weak non-Hermiticity [53], where the symmetry parameter scales with N as $\eta = 1 - \mathcal{O}(1/N)$, the number of real eigenvalues of J remains proportional to N ($N \gg 1$) [46]. This implies

that the complexity of the configuration space characterizing the symmetric spherical model remains essentially unchanged under the introduction of a sufficiently weak antisymmetric perturbation. Hence, in this weakly non-Hermitian regime, the two-time observables of the spherical model with non-reciprocal interactions are expected to exhibit slow dynamics. Understanding the dynamics of the spherical model in this regime is therefore an interesting problem that we will address in a future work. It would be also important to clarify whether complex systems governed by nonlinear and asymmetric interactions [3, 1, 4, 8], such as neural networks and ecosystems, can display nontrivial dynamical properties, including the breakdown of time-translation invariance and aging.

Acknowledgments

F. L. M. acknowledges a visiting researcher fellowship from FAPERJ (Grant No 204.646/2024) and financial support from CNPq (Grants No 402487/2023-0 and No 310255/2025-2). F. L. M. warmly thanks the hospitality of the Physics Institute of the Fluminense Federal University, where this work has been developed. D. A. S. acknowledges financial support from CNPq (Grants CNPq/MCTI No 10/2023, No 402487/2023-0 and CNPq No 4/2021, No 307337/2021-9).

Appendix A. The correlation and response functions for a finite system

In this appendix we show the main steps in the derivation of the finite-size expressions for the correlation and response functions, Eqs. (17) and (18), which are valid for arbitrary interaction matrix J and initial conditions. This is achieved by solving the coupled system of Eqs. (12) and (13) for the projections $r_{\alpha}(t) = \langle S(t)|R_{\alpha}\rangle$ and $l_{\alpha}(t) = \langle S(t)|L_{\alpha}\rangle$. The solution of Eq. (12) is given by

$$r_{\alpha}(t) = r_{\alpha}(0)\Gamma_{h}(t)e^{\lambda_{\alpha}t} + e^{\lambda_{\alpha}t}\Gamma_{h}(t)\int_{0}^{t} dt' \frac{h_{\alpha}^{(R)}(t')}{\Gamma_{h}(t')}e^{-\lambda_{\alpha}t'}, \tag{A.1}$$

where we introduced the function

$$\Gamma_h(t) = \exp\left[-\int_0^t dt' z(t')\right]. \tag{A.2}$$

Our notation highlights that $\Gamma_h(t)$ depends on the external fields $\{h_i(t)\}_{i=1}^N$, which will be important in the calculation of the response function. Inserting the above solution for $r_{\alpha}(t)$ in Eq. (13), we obtain

$$\frac{\partial l_{\alpha}(t)}{\partial t} = -z(t)l_{\alpha}(t) + F_{\alpha}(t), \tag{A.3}$$

with

$$F_{\alpha}(t) = \sum_{\beta=1}^{N} \lambda_{\beta} \langle L_{\beta} | L_{\alpha} \rangle \Gamma_{h}(t) e^{\lambda_{\beta} t} \left[r_{\beta}(0) + \int_{0}^{t} ds \, \frac{h_{\beta}^{(R)}(s)}{\Gamma_{h}(s)} e^{-\lambda_{\beta} s} \right] + h_{\alpha}^{(L)}(t). \tag{A.4}$$

Equation (A.3) is a linear dynamical equation with an additive noise $F_{\alpha}(t)$ generated by the time evolution of the amplitudes $r_{\alpha}(t)$. The overlap $\langle L_{\beta}|L_{\alpha}\rangle$ in Eq. (A.4) couples the dynamics of $l_{\alpha}(t)$ with the whole set of right eigenvectors, which is a direct consequence of the non-orthogonality of the eigenvectors. The solution of Eq. (A.3) reads

$$l_{\alpha}(t) = l_{\alpha}(0)\Gamma_{h}(t) + \Gamma_{h}(t) \int_{0}^{t} dt' \frac{F_{\alpha}(t')}{\Gamma_{h}(t')}.$$
(A.5)

Substituting Eq. (A.4) in the above expression and using the property $l_{\alpha}(0) = \sum_{\beta=1}^{N} r_{\beta}(0) \langle L_{\beta} | L_{\alpha} \rangle$, we find

$$l_{\alpha}(t) = \Gamma_{h}(t) \sum_{\beta=1}^{N} r_{\beta}(0) \langle L_{\beta} | L_{\alpha} \rangle e^{\lambda_{\beta} t} + \Gamma_{h}(t) \sum_{\beta=1}^{N} \lambda_{\beta} \langle L_{\beta} | L_{\alpha} \rangle \int_{0}^{t} dt' e^{\lambda_{\beta} t'} U_{\beta}(t'|h)$$

$$+ \Gamma_{h}(t) \int_{0}^{t} dt' \frac{h_{\alpha}^{(L)}(t')}{\Gamma_{h}(t')}, \tag{A.6}$$

where

$$U_{\beta}(t|h) = \int_0^t ds \, \frac{h_{\beta}^{(R)}(s)}{\Gamma_h(s)} e^{-\lambda_{\beta} s}. \tag{A.7}$$

The solutions for $r_{\alpha}(t)$ and $l_{\alpha}(t)$, Eqs. (A.1) and (A.6), are determined by the external fields and $\Gamma_h(t)$. Thus, in order to close the system of equations, we need an equation for $\Gamma_h(t)$. Substituting Eqs. (A.1) and (A.6) in the spherical constraint

$$\sum_{\alpha=1}^{N} r_{\alpha}(t) l_{\alpha}^{*}(t) = N, \tag{A.8}$$

we obtain an explicit equation for $\Gamma_h(t)$,

$$\frac{N}{\Gamma_h^2(t)} = \sum_{\alpha\beta=1}^N r_\alpha(0) r_\beta^*(0) \langle L_\beta | L_\alpha \rangle^* e^{\lambda_\alpha t + \lambda_\beta^* t} + \sum_{\alpha\beta=1}^N r_\alpha(0) \lambda_\beta^* e^{\lambda_\alpha t} \langle L_\beta | L_\alpha \rangle^* \int_0^t ds e^{\lambda_\beta^* s} U_\beta^*(s|h)
+ \sum_{\alpha=1}^N r_\alpha(0) e^{\lambda_\alpha t} \int_0^t ds \frac{\left(h_\alpha^{(L)}(s)\right)^*}{\Gamma_h(s)} + \sum_{\alpha\beta=1}^N r_\beta^*(0) \langle L_\beta | L_\alpha \rangle^* e^{\lambda_\alpha t + \lambda_\beta^* t} U_\alpha(t|h)
+ \sum_{\alpha\beta=1}^N \lambda_\beta^* e^{\lambda_\alpha t} \langle L_\beta | L_\alpha \rangle^* U_\alpha(t|h) \int_0^t ds e^{\lambda_\beta^* s} U_\beta^*(s|h)
+ \sum_{\alpha=1}^N e^{\lambda_\alpha t} U_\alpha(t|h) \int_0^t ds \frac{\left(h_\alpha^{(L)}(s)\right)^*}{\Gamma_h(s)}.$$
(A.9)

The solutions of Eqs. (A.1), (A.6) and (A.9) determine the time evolution of the projections, $\{r_{\alpha}(t)\}_{\alpha=1}^{N}$ and $\{l_{\alpha}(t)\}_{\alpha=1}^{N}$, from which one can compute the correlation and response functions.

Although we are not interested in the effects of the external fields on the dynamics, the generic form of Eq. (A.9) for arbitrary $\{h_i(t)\}_{i=1}^N$ is crucial to compute the response function, given by Eq. (16). The derivative $\frac{\delta r_{\alpha}(t)}{\delta h_i(t')}\Big|_{h=0}$ of Eq. (A.1) reads

$$\frac{\delta r_{\alpha}(t)}{\delta h_{i}(t')}\Big|_{h=0} = r_{\alpha}(0)e^{\lambda_{\alpha}t} \frac{\delta \Gamma_{h}(t)}{\delta h_{i}(t')}\Big|_{h=0} + \frac{\Gamma_{0}(t)}{\Gamma_{0}(t')}e^{\lambda_{\alpha}(t-t')} \langle i|R_{\alpha}\rangle \quad (t' < t), \tag{A.10}$$

where $\Gamma_0(t) = \lim_{h\to 0} \Gamma_h(t)$ fulfills

$$\frac{N}{\Gamma_0^2(t)} = \sum_{\alpha\beta=1}^N r_\alpha(0) r_\beta^*(0) \langle L_\beta | L_\alpha \rangle^* e^{\lambda_\alpha t + \lambda_\beta^* t}.$$
 (A.11)

An explicit expression for $\frac{\delta\Gamma_h(t)}{\delta h_i(t')}\Big|_{t=0}$ is obtained from Eq. (A.9), namely

$$\frac{\delta\Gamma_h(t)}{\delta h_i(t')}\Big|_{h=0} = -\frac{1}{N} \frac{\Gamma_0^3(t)}{\Gamma_0(t')} \operatorname{Re} \left[\sum_{\alpha\beta=1}^N r_\alpha(0) \left\langle L_\alpha | L_\beta \right\rangle \left\langle R_\beta | i \right\rangle e^{\lambda_\alpha t + \lambda_\beta^*(t-t')} \right] . (A.12)$$

Combining Eqs. (16), (A.10) and (A.12), we arrive at the following expression

$$G_N(t,t') = \frac{\Gamma_0(t)}{\Gamma_0(t')} \frac{1}{N} \sum_{\alpha=1}^N e^{\lambda_\alpha(t-t')}$$

$$- \frac{\Gamma_0^3(t)}{\Gamma_0(t')} \operatorname{Re} \left[\frac{1}{N^2} \sum_{\alpha\beta=1}^N r_\alpha(0) r_\beta^*(0) \left\langle L_\alpha | L_\beta \right\rangle e^{\lambda_\alpha t + \lambda_\beta^*(2t-t')} \right]$$
(A.13)

for the response function of finite-size systems. It is easier to derive an equation for the correlation function $C_N(t, t')$ in the absence of external fields. Setting $h_i(t) = 0$ in Eqs. (A.1) and (A.6), and substituting them in Eq. (15), we get

$$C_N(t,t') = \Gamma_0(t)\Gamma_0(t')\frac{1}{N}\sum_{\alpha\beta=1}^N r_\alpha(0)r_\beta^*(0) \langle L_\alpha|L_\beta\rangle e^{\lambda_\alpha t + \lambda_\beta^* t'}.$$
 (A.14)

By introducing the two-time function $W_N(t,t')$, defined in Eq. (19), the above expressions for $G_N(t,t')$ and $C_N(t,t')$ lead to Eqs. (17) and (18) in the main text.

References

- [1] A. Crisanti and H. Sompolinsky, "Path integral approach to random neural networks," *Phys. Rev.* E, vol. 98, p. 062120, Dec 2018.
- [2] D. Martí, N. Brunel, and S. Ostojic, "Correlations between synapses in pairs of neurons slow down dynamics in randomly connected neural networks," *Phys. Rev. E*, vol. 97, p. 062314, Jun 2018.
- [3] G. Bunin, "Ecological communities with lotka-volterra dynamics," *Phys. Rev. E*, vol. 95, p. 042414, Apr 2017.
- [4] F. Roy, G. Biroli, G. Bunin, and C. Cammarota, "Numerical implementation of dynamical mean field theory for disordered systems: application to the lotka-volterra model of ecosystems," *Journal of Physics A: Mathematical and Theoretical*, vol. 52, p. 484001, nov 2019.
- [5] A. Altieri, F. Roy, C. Cammarota, and G. Biroli, "Properties of equilibria and glassy phases of the random lotka-volterra model with demographic noise," *Phys. Rev. Lett.*, vol. 126, p. 258301, Jun 2021.
- [6] R. Pastor-Satorras, C. Castellano, P. Van Mieghem, and A. Vespignani, "Epidemic processes in complex networks," Rev. Mod. Phys., vol. 87, pp. 925–979, Aug 2015.
- [7] T. M. Pham and K. Kaneko, "Dynamical theory for adaptive systems," Journal of Statistical Mechanics: Theory and Experiment, vol. 2024, p. 113501, nov 2024.
- [8] F. L. Metz, "Dynamical mean-field theory of complex systems on sparse directed networks," Phys. Rev. Lett., vol. 134, p. 037401, Jan 2025.
- [9] C. De Dominicis and I. Giardina, Random Fields and Spin Glasses: A Field Theory Approach. Cambridge University Press, 2006.

- [10] L. F. Cugliandolo, "Dynamics of glassy systems," in *Slow relaxations and non-equilibrium dynamics in condensed matter* (F. M. V. Barrat J L, Kurchan J and D. J, eds.), Springer-Verlag, 2003.
- [11] Y. V. Fyodorov, E. Gudowska-Nowak, M. A. Nowak, and W. Tarnowski, "Nonorthogonal eigenvectors, fluctuation-dissipation relations, and entropy production," *Phys. Rev. Lett.*, vol. 134, p. 087102, Feb 2025.
- [12] G. Livan, M. Novaes, and P. Vivo, *Introduction to Random Matrices: Theory and Practice*. SpringerBriefs in Mathematical Physics, Springer International Publishing, 2018.
- [13] L. F. Cugliandolo and D. S. Dean, "Full dynamical solution for a spherical spin-glass model," *J. Phys. A: Math. Gen.*, vol. 28, pp. 4213–4234, aug 1995.
- [14] M. Henkel, "Physical ageing from generalised time-translation-invariance," Nuclear Physics B, vol. 1017, p. 116968, 2025.
- [15] J. Kurchan and L. Laloux, "Phase space geometry and slow dynamics," *Journal of Physics A: Mathematical and General*, vol. 29, p. 1929, may 1996.
- [16] A. V. Ivlev, J. Bartnick, M. Heinen, C.-R. Du, V. Nosenko, and H. Löwen, "Statistical mechanics where newton's third law is broken," *Phys. Rev. X*, vol. 5, p. 011035, Mar 2015.
- [17] M. Fruchart, R. Hanai, P. B. Littlewood, and V. Vitelli, "Non-reciprocal phase transitions," *Nature*, vol. 592, no. 7854, pp. 363–369, 2021.
- [18] D. Martin and et al., "Non-reciprocity across scales in active mixtures," Nature Physics, vol. 19, pp. 1545–1552, 2023.
- [19] C. Martorell, R. Calvo, A. Annibale, and M. A. Muñoz, "Dynamically selected steady states and criticality in non-reciprocal networks," *Chaos, Solitons & Fractals*, vol. 182, p. 114809, 2024.
- [20] E. Blumenthal, J. W. Rocks, and P. Mehta, "Phase transition to chaos in complex ecosystems with nonreciprocal species-resource interactions," *Phys. Rev. Lett.*, vol. 132, p. 127401, Mar 2024.
- [21] V. Ros, F. Roy, G. Biroli, G. Bunin, and A. M. Turner, "Generalized lotka-volterra equations with random, nonreciprocal interactions: The typical number of equilibria," *Phys. Rev. Lett.*, vol. 130, p. 257401, Jun 2023.
- [22] A. Bhattacherjee, Y. Hayakawa, and T. Shibata, "Structure formation induced by non-reciprocal cell-cell interactions in a multicellular system," *Soft Matter*, vol. 20, pp. 2931–2942, 2024.
- [23] J. Garnier-Brun, M. Benzaquen, and J.-P. Bouchaud, "Unlearnable games and "satisficing" decisions: A simple model for a complex world," *Phys. Rev. X*, vol. 14, p. 021039, Jun 2024.
- [24] R. Hanai, "Nonreciprocal frustration: Time crystalline order-by-disorder phenomenon and a spin-glass-like state," *Phys. Rev. X*, vol. 14, p. 011029, Feb 2024.
- [25] G. Garcia Lorenzana, A. Altieri, G. Biroli, M. Fruchart, and V. Vitelli, "Nonreciprocal spin-glass transition and aging," *Phys. Rev. Lett.*, vol. 135, p. 187402, Oct 2025.
- [26] G. G. Lorenzana, D. Martin, Y. Avni, D. S. Seara, M. Fruchart, G. Biroli, and V. Vitelli, "When is nonreciprocity relevant?," preprint arXiv:2509.17972, 2025.
- [27] D. Badalotti, C. Baldassi, M. Mézard, M. Scardecchia, and R. Zecchina, "Dynamical learning in deep asymmetric recurrent neural networks," preprint arXiv:2509.05041, 2025.
- [28] A. Mahadevan and D. S. Fisher, "Continual evolution in nonreciprocal ecological models," *PRX Life*, vol. 3, p. 033008, Aug 2025.
- [29] L. Guislain and E. Bertin, "Far-from-equilibrium complex landscapes," Phys. Rev. E, vol. 111, p. L062101, Jun 2025.
- [30] G. Garcia Lorenzana, A. Altieri, G. Biroli, M. Fruchart, and V. Vitelli, "Nonreciprocally coupled spin glasses: Exceptional-point-mediated phase transitions and aging," *Phys. Rev. E*, vol. 112, p. 044154, Oct 2025.
- [31] Y. Ashida, Z. Gong, and M. Ueda, "Non-hermitian physics," *Advances in Physics*, vol. 69, no. 3, pp. 249–435, 2020.
- [32] Q.-B. Zeng and R. Lü, "Real spectra and phase transition of skin effect in nonreciprocal systems," *Physical Review B*, vol. 105, 06 2022.
- [33] N. Okuma and M. Sato, "Non-hermitian topological phenomena: A review," *Annual Review of Condensed Matter Physics*, vol. 14, no. Volume 14, 2023, pp. 83–107, 2023.

- [34] G. Kennedy, "Quantum torque on a non-reciprocal body out of thermal equilibrium and induced by a magnetic field of arbitrary strength," *The European Physical Journal Special Topics*, vol. 232, pp. 3197–3208, 2023.
- [35] S. Begg, R. Hanai, et al., "Quantum criticality in open quantum spin chains with nonreciprocity," Physical Review Letters, vol. 132, no. 12, p. 120401, 2024.
- [36] Z.-T. Cai, H.-D. Li, and W. Chen, "Quantum-classical correspondence of non-hermitian symmetry breaking," *Phys. Rev. Lett.*, vol. 134, p. 240201, Jun 2025.
- [37] H. Sompolinsky, A. Crisanti, and H. J. Sommers, "Chaos in random neural networks," Phys. Rev. Lett., vol. 61, pp. 259–262, Jul 1988.
- [38] A. Crisanti and H. Sompolinsky, "Dynamics of spin systems with randomly asymmetric bonds: Langevin dynamics and a spherical model," *Phys. Rev. A*, vol. 36, p. 4922, 1987.
- [39] L. F. Cugliandolo, K. J., P. Le Doussal, and L. Peliti, "Glassy behaviour in disordered systems with nonrelaxational dynamics," *Phys. Rev. Lett.*, vol. 78, p. 350, 1997.
- [40] G. Iori and E. Marinari, "On the stability of the mean-field spin glass broken phase under non-hamiltonian perturbations," *Journal of Physics A: Mathematical and General*, vol. 30, p. 4489, jul 1997.
- [41] E. Marinari and D. A. Stariolo, "Off-equilibrium dynamics of a four-dimensional spin glass with asymmetric couplings," *Journal of Physics A: Mathematical and General*, vol. 31, p. 5021, jun 1998.
- [42] L. Berthier and K. J., "Non-equilibrium glass transitions in driven and active matter," *Nature Phys*, vol. 9, pp. 310–314, 2013.
- [43] J. T. Chalker and B. Mehlig, "Eigenvector statistics in non-hermitian random matrix ensembles," *Phys. Rev. Lett.*, vol. 81, pp. 3367–3370, Oct 1998.
- [44] B. Mehlig and J. T. Chalker, "Statistical properties of eigenvectors in non-hermitian gaussian random matrix ensembles," *Journal of Mathematical Physics*, vol. 41, pp. 3233–3256, 05 2000.
- [45] T. R. Würfel, M. J. Crumpton, and Y. V. Fyodorov, "Mean left-right eigenvector self-overlap in the real ginibre ensemble," *Random Matrices: Theory and Applications*, vol. 13, no. 04, p. 2450017, 2024.
- [46] M. J. Crumpton, Y. V. Fyodorov, and T. R. Würfel, "Mean eigenvector self-overlap in the real and complex elliptic ginibre ensembles at strong and weak non-hermiticity," Ann. Henri Poincaré, vol. 26, p. 2069, 2025.
- [47] H. J. Sommers, A. Crisanti, H. Sompolinsky, and Y. Stein, "Spectrum of large random asymmetric matrices," Phys. Rev. Lett., vol. 60, pp. 1895–1898, May 1988.
- [48] V. L. Girko, "Elliptic law," Theory of Probability & Its Applications, vol. 30, no. 4, pp. 677–690, 1986.
- [49] P. Bourgade and G. Dubach, "The distribution of overlaps between eigenvectors of ginibre matrices," Probab. Theory Relat. Fields, vol. 177, p. 397, 2020.
- [50] P. J. Forrester and T. Nagao, "Skew orthogonal polynomials and the partly symmetric real ginibre ensemble," *Journal of Physics A: Mathematical and Theoretical*, vol. 41, p. 375003, aug 2008.
- [51] S.-S. Byun, N.-G. Kang, J. O. Lee, and J. Lee, "Real eigenvalues of elliptic random matrices," *International Mathematics Research Notices*, vol. 2023, pp. 2243–2280, 11 2021.
- [52] Y. V. Fyodorov, "Topology trivialization transition in random non-gradient autonomous odes on a sphere," *Journal of Statistical Mechanics: Theory and Experiment*, vol. 2016, p. 124003, dec 2016.
- [53] Y. V. Fyodorov, B. A. Khoruzhenko, and H.-J. Sommers, "Almost hermitian random matrices: Crossover from wigner-dyson to ginibre eigenvalue statistics," *Phys. Rev. Lett.*, vol. 79, pp. 557–560, Jul 1997.